

EUROPEAN  
HEMATOLOGY  
ASSOCIATIONFerrata Storti  
Foundation

# Endothelin type A receptors mediate pain in a mouse model of sickle cell disease

Brianna Marie Lutz,<sup>1,2</sup> Shaogen Wu,<sup>1</sup> Xiyao Gu,<sup>1</sup> Fidelis E. Atianjoh,<sup>1,3</sup> Zhen Li,<sup>1</sup> Brandon M. Fox,<sup>4</sup> David M. Pollock<sup>4</sup> and Yuan-Xiang Tao<sup>1,2,5</sup>

<sup>1</sup>Department of Anesthesiology, New Jersey Medical School, Rutgers, The State University of New Jersey, Newark, NJ, USA; <sup>2</sup>Rutgers Graduate School of Biomedical Sciences, New Jersey Medical School, The State University of New Jersey, Newark, NJ, USA; <sup>3</sup>Intensive Care Unit, MedStar Southern Maryland Hospital Center, Clinton, MD, USA; <sup>4</sup>Cardio-Renal Physiology and Medicine, Department of Medicine, University of Alabama at Birmingham, AL, USA and <sup>5</sup>Neuroscience Research Institute, Zhengzhou University Academy of Medical Sciences, Henan, China

**Haematologica** 2018  
Volume 103(7):1124-1135

## ABSTRACT

Sickle cell disease is associated with acute painful episodes and chronic intractable pain. Endothelin-1, a known pain inducer, is elevated in the blood plasma of both sickle cell patients and mouse models of sickle cell disease. We show here that the levels of endothelin-1 and its endothelin type A receptor are increased in the dorsal root ganglia of a mouse model of sickle cell disease. Pharmacologic inhibition or neuron-specific knockdown of endothelin type A receptors in primary sensory neurons of dorsal root ganglia alleviated basal and post-hypoxia evoked pain hypersensitivities in sickle cell mice. Mechanistically, endothelin type A receptors contribute to sickle cell disease-associated pain likely through the activation of NF- $\kappa$ B-induced Nav1.8 channel upregulation in primary sensory neurons of sickle cell mice. Our findings suggest that endothelin type A receptor is a potential target for the management of sickle cell disease-associated pain, although this expectation needs to be further verified in clinical settings.

## Correspondence:

yt211@njms.rutgers.edu

Received: December 21, 2017.

Accepted: March 13, 2018.

Pre-published: March 15, 2018.

doi:10.3324/haematol.2017.187013

Check the online version for the most updated information on this article, online supplements, and information on authorship & disclosures: [www.haematologica.org/content/103/7/1124](http://www.haematologica.org/content/103/7/1124)

©2018 Ferrata Storti Foundation

Material published in *Haematologica* is covered by copyright. All rights are reserved to the Ferrata Storti Foundation. Use of published material is allowed under the following terms and conditions:

<https://creativecommons.org/licenses/by-nc/4.0/legalcode>.

Copies of published material are allowed for personal or internal use. Sharing published material for non-commercial purposes is subject to the following conditions:

<https://creativecommons.org/licenses/by-nc/4.0/legalcode>,

sect. 3. Reproducing and sharing published material for commercial purposes is not allowed without permission in writing from the publisher.



## Introduction

Sickle cell disease (SCD) results from an amino acid substitution in the  $\beta$  globin chain of the oxygen carrying molecule, hemoglobin.<sup>1</sup> Approximately 100,000 Americans currently suffer from SCD, and over 80,000 SCD related hospitalizations occur annually resulting in over 450 million dollars in healthcare costs.<sup>2</sup> Much of these healthcare costs and hospitalizations stem from acute vaso-occlusive episodes in which patients often report extreme pain.<sup>3</sup> Pain is a hallmark of SCD and correlates with morbidity and disease severity.<sup>4</sup> In addition to acute painful episodes, some SCD patients report persistent/chronic pain.<sup>5</sup> Treatment for SCD-associated pain includes pain medications such as opioids, but pain relief may remain inadequate for many SCD patients. Additionally, repeated and/or prolonged administration of these drugs has potential side effects.<sup>6</sup> Understanding the causes of pain in SCD may bring forward new and more efficient therapeutic strategies for the management of SCD pain.

Endothelin-1 (ET-1) is a 21 amino acid peptide released from endothelial cells, immune cells, and neurons.<sup>7</sup> ET-1 binds to endothelin type A (ET<sub>A</sub>) and endothelin type B (ET<sub>B</sub>) G-protein coupled receptors.<sup>7</sup> Classically, ET-1 acts as a vaso-constrictor, but recent studies have shown that ET-1 can also induce pain in humans and rodents.<sup>8,9</sup> In the dorsal root ganglia (DRG), ET<sub>A</sub> receptors are expressed predominantly in the primary sensory neurons, while ET<sub>B</sub> receptors are detected in glial cells.<sup>10</sup> Blocking ET<sub>A</sub> receptors attenuates ET-1-induced nerve fiber activation and pain behavior in rodents.<sup>7,11,12</sup> ET-1-induced activation of the ET<sub>A</sub> receptor has been found to increase intracellular calcium release, potentiate transient receptor potential vanilloid 1 current, and alter the functioning of tetrodotoxin-resistant (TTX-R) sodium channels in DRG neurons,<sup>8</sup> but detailed mechanisms of how ET-1 induces pain are not fully understood.

In SCD patients, blood plasma ET-1 levels are elevated at a basal level and increase further during an acute vaso-occlusive crisis.<sup>13,14</sup> Elevated ET-1 and its subsequent activation of ET<sub>A</sub> receptors have been demonstrated to contribute to SCD pathology, including renal injury<sup>15</sup> and pulmonary hypertension.<sup>16</sup> The level of ET-1 mRNA is also increased in the DRG of SCD mice.<sup>17</sup> However, whether and how this elevated ET-1 in SCD DRG contributes to SCD-associated pain remains elusive. Given that ET<sub>A</sub> receptor antagonists have been used in phase II/III clinical trials for cancer treatment<sup>18,19</sup> and SCD-related pulmonary hypertension,<sup>16</sup> identifying the role of ET-1 and its ET<sub>A</sub> receptors in SCD-associated pain may provide a new avenue for treatment of SCD-associated pain in patients.

Humanized mouse models of SCD display persistent pain hypersensitivity that can worsen with exposure to hypoxia.<sup>17,20,21</sup> In the present study, using the humanized Townes (HbSS) and Berkeley (BerkSS) mouse models of SCD, we first examined whether local pharmacologic inhibition or conditional knockout of ET<sub>A</sub> receptors in DRG neurons affected pain hypersensitivity in SCD mice. We then examined whether SCD mice expressed elevated levels of ET-1 and ET<sub>A</sub> receptors in DRG neurons. Finally, we unveiled a possible molecular mechanism by which DRG ET<sub>A</sub> receptors mediate SCD pain through the activation of NF- $\kappa$ B and subsequent increase of Nav1.8 expression in the DRG.

## Methods

### Animals

All procedures used in this study have been approved by the Rutgers New Jersey Medical School Animal Care and Use Committee and adhere to the ethical guidelines of the National Institutes of Health and the International Association for the Study of Pain. All experiments were designed to minimize animal suffering and the number of animals used, and were conducted in a blind manner. Detailed animal information can be found in *Online Supplementary Methods*.

### Behavioral analysis

Mechanical testing, thermal testing, and cold testing were conducted on the same day with at least 1 hour rest periods between tests as described.<sup>22</sup> The conditioned place-preference (CPP) test was carried out as described<sup>22</sup> and in the *Online Supplementary Methods*.

### Hypoxia/Reoxygenation

Hypoxia/reoxygenation exposure for the induction of vaso-occlusion was conducted in the same manner as previously described.<sup>20</sup> The detailed procedures can be found in the *Online Supplementary Methods*.

### Genetic Knockdown and Bone Marrow Transplantation

Chimeric mouse generation was completed using a previously described protocol, which showed the development of the sickle cell phenotype in BerkSS bone marrow-recipient mice beginning at 2 months after transplantation.<sup>23</sup> The detailed procedures can be found in the *Online Supplementary Methods*.

Isoelectric focusing, cell culture, immunofluorescence, Western blotting, qRT-PCR, ChIP assay, luciferase assay, electrophysiological recording, and statistical analysis methods can be found in the *Online Supplementary Methods*.

## Results

### Pain hypersensitivity in SCD mouse models

We first characterized basal pain behaviors in our colony of Townes humanized SCD mice. HbSS and HbAA mice (as a control) aged 4-6 months were used. Like male BerkSS mice (*Online Supplementary Figure S2A, B*), male HbSS mice displayed significant bilateral increases in basal paw withdrawal frequencies (PWF) in response to 0.16 g and 0.4 g von Frey filaments (Figure 1 A, B), and reductions in paw withdrawal latencies (PWL) to both thermal and cold stimuli when compared to their HbAA littermates (Figure 1 C, D). Similar pain hypersensitivities were seen in female HbSS mice (*Online Supplementary Figure S3 A-D*).

We then examined whether pain hypersensitivities stemmed from an increase in DRG neuronal excitability in HbSS mice. Compared to HbAA mice, the medium and small DRG neurons of HbSS mice showed increases of 9.85 mV and 8.24 mV, respectively, in the resting membrane potentials (Figure 2A) and decreases of 36% and 52%, respectively, in the current thresholds for action potential generation (Figure 2B). The number of action potentials evoked by a stimulation of  $\geq 200$  pA in medium and small neurons was significantly higher in HbSS mice (Figure 2C, D), although both mice displayed similar membrane input resistances and other action potential parameters, (*Online Supplementary Table S1*). In addition, a larger percentage of small and medium HbSS DRG neurons exhibited spontaneous activity compared to HbAA DRG neurons (Figure 2 E, F). The frequency of spontaneous action potential generation was also higher in HbSS small and medium DRG neurons compared to HbAA neurons (Figure 2 G). These indicators of heightened excitability were not seen in large DRG neurons (Figure 2 A-G).

### Effect of DRG ET<sub>A</sub> receptor inhibition on SCD pain

To address the role of DRG ET<sub>A</sub> receptors in SCD-associated pain, we subcutaneously (s.c.) injected ABT-627, a selective and specific ET<sub>A</sub> receptor antagonist,<sup>24</sup> into the plantar side of the left hindpaw. Single administration of 5 nmol ABT-627, 2 hours before behavioral testing under normoxic conditions, led to the attenuation of ipsilateral mechanical (Figure 3A, B; *Online Supplementary Figure S3A, B*), thermal (Figure 3C; *Online Supplementary Figure S3C*) and cold (Figure 3D; *Online Supplementary Figure S3D*) pain hypersensitivities in the male and female HbSS mice. This effect is dose-dependent (*Online Supplementary Figure S4*). ABT-627 did not alter the basal mechanical, thermal and cold responses of the male and female HbAA mice (Figure 3 A-D; *Online Supplementary Figure S3 A-D*). Similar ABT-627 efficacy was evident in male BerkSS mice (*Online Supplementary Figure S2 A-D*).

Exposure to hypoxia/reoxygenation in SCD mice has been implicated as a method of inducing vaso-occlusion and mimicking acute painful episodes in SCD patients.<sup>20</sup> We further performed behavior analyses following hypoxia/reoxygenation exposure in SCD mice. Male HbSS mice exhibited similar responses to the 0.4 g von Frey filament (Figure 3B), thermal (Figure 3C), and cold (Figure 3D) stimuli before and after hypoxia/reoxygenation. However, after hypoxia/reoxygenation, bilateral PWF to the 0.16 g von Frey filament increased by 20% in male HbSS mice compared to basal values (Figure 3A). ABT-627 administered to the unilateral hind paw immediately after hypox-

ia exposure, led to the attenuation of ipsilateral mechanical, thermal, and cold pain hypersensitivities in male HbSS mice (Figure 3 A-D), although it did not affect basal or post-hypoxia ipsilateral responses in HbAA mice (Figure 3A-D) or contralateral responses in HbAA and HbSS mice (Online Supplementary Figure S5). Similar ABT-627 efficacy was seen in male BerkSS mice after hypoxia/reoxygenation exposure (Online Supplementary Figure S6 A-D). There were no sex-based differences in pain hypersensitivities and ABT-627 efficacy after hypoxia/reoxygenation exposure (Figure 3 A-D, Online Supplementary Figure S7).

Spontaneous ongoing pain in HbSS mice using a CPP paradigm was also examined. HbSS mice, but not HbAA mice, given vehicle once a day for 4 days prior to and during CPP testing (Online Supplementary Figure S1), spent significantly more time in the lidocaine-paired chamber after conditioning compared to their pre-test time (Figure 3 E, F). When given ABT-627 systemically (i.p) once a day for four days prior to and during testing (Online Supplementary Figure S1), neither HbSS nor HbAA mice displayed a significant lidocaine-paired chamber preference (Figure 3 E, F).

### Effect of knockdown of DRG $ET_A$ receptors on SCD pain

The effects of ABT-627 hindpaw administration described above suggest the role of peripheral  $ET_A$  receptors in SCD-associated pain; however, ABT-627 lacks cell-type specificity and may also have off-target effects. As a complementary approach, we generated a DRG neuron-specific  $ET_A$  receptor knockout mouse by crossing an  $ET_A^{flax/flax}$  mouse with an Advillin<sup>cre/+</sup> mouse in which Cre-recombinase is expressed only in Advillin-positive neurons exclusive to the DRG and trigeminal ganglia. DRG-

specific knockdown of  $ET_A$  receptors was validated using Western blotting and immunostaining (Online Supplementary Figure S8 A, B). Two months after bone marrow transplantation, donor hemoglobin expression in the recipient mice was confirmed using isoelectric focusing (Online Supplementary Figure S8 C). Mice receiving BerkSS bone marrow only expressed human  $\beta$ s globin ( $\beta$ SS). BerkAA bone marrow recipients expressed the normal human  $\beta$  globin ( $\beta$ AA; Online Supplementary Figure S8 C) and were used as a control. Mouse hemoglobin (Hb) was not found in the blood of recipient mice (Online Supplementary Figure S8 C), confirming the knockdown of mouse globin.

Bilateral evoked pain hypersensitivities as evidenced by the increase in PWF to mechanical stimuli and the decrease in PWL to thermal and cold stimuli developed in the  $ET_A^{flax/flax}$  mice expressing  $\beta$ SS (Figure 4 A-D) 2 months after bone marrow transplantation. These pain hypersensitivities had a tendency of aggravation after hypoxia/reoxygenation (Figure 4 A-D).  $ET_A^{cre/flax}$  mice expressing  $\beta$ SS failed to develop these pain hypersensitivities after bone marrow transplantation in both normoxic and post-hypoxia/reoxygenation conditions (Figure 4 A-D).  $ET_A^{flax/flax}$  mice and  $ET_A^{cre/flax}$  mice transplanted with normal human  $\beta$ AA maintained normal basal responses after bone marrow transplantation under normoxia and hypoxia/reoxygenation conditions (Figure 4 A-D).

### Increased ET-1 and $ET_A$ receptor expression in SCD DRG

Our behavioral observations indicate the significance of DRG  $ET_A$  receptors in pain hypersensitivity in HbSS mice. We next examined the expression of the  $ET_A$  receptor and

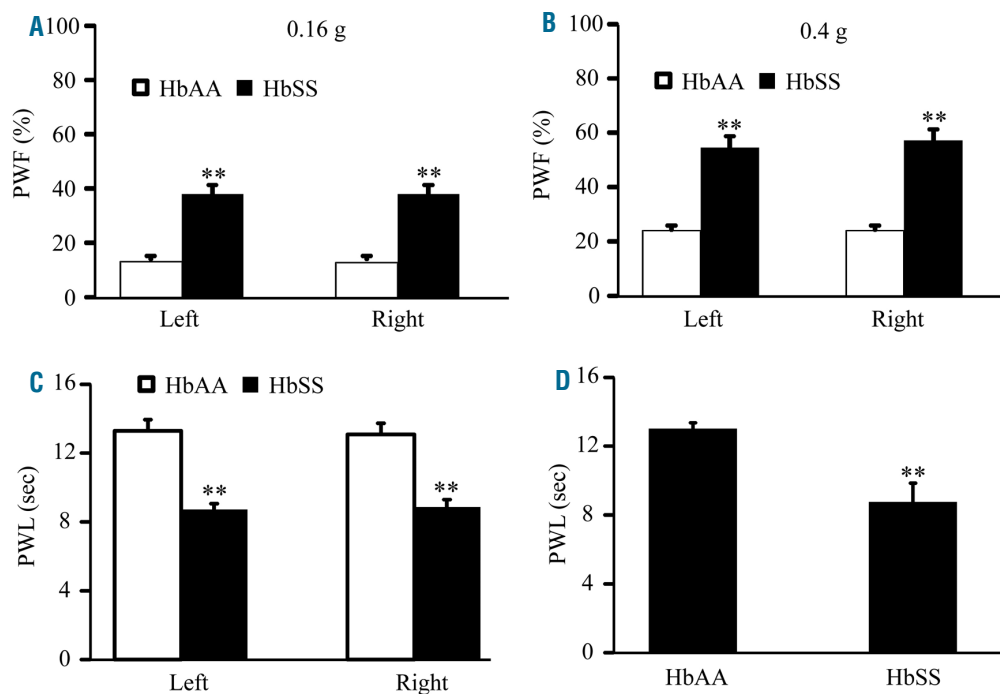


**Figure 1. Male Townnes HbSS mice display evoked pain hypersensitivity.** Paw withdrawal frequencies (PWF) to a 0.16 g low force (A) and a 0.4 g medium force (B) von Frey filaments and paw withdrawal latencies (PWL) to thermal (C) and cold (D) stimuli on both left and right hind paws of 4 month old male HbAA and HbSS mice. n = 10 mice/genotype, \*\*P < 0.01 vs. the corresponding HbAA group.

its ligand, ET-1, in the DRG and peripheral tissue of HbSS mice. *Edn1* mRNA (encoding ET1) and ET-1 protein were elevated in HbSS mouse DRG (Figure 5 A, B). *Ednra* mRNA (encoding ET<sub>A</sub> receptor) expression in the DRG did not differ between HbAA and HbSS mice, but the level of ET<sub>A</sub> receptor protein significantly increased in HbSS DRG (Figure 5 A, B). In accordance with previous studies,<sup>10,25</sup> ET<sub>A</sub> receptors were expressed exclusively in the neurons of DRG. Approximately 43% of ET<sub>A</sub> receptor-labeled neurons are positive for CGRP, 36% for IB4, and only 12% for NF200 (Figure 5 C). Interestingly, the immunostaining for pre-pro ET-1, a precursor of ET-1 peptide, was also restricted to DRG neurons (*Online Supplementary Figure S9*). About 36% of pre-pro ET-1-labeled neurons are positive for CGRP, 56% for IB4, and 7% for NF200 (Figure 5C). The percentage of neurons expressing ET<sub>A</sub> receptors or pre-pro ET-1 within the DRG of HbSS mice was 45% and 32%, respectively, higher than those in the HbAA DRG (Figure 5 D, E). Unexpectedly, there was no significant difference in hindpaw expression of ET-1 or ET<sub>A</sub> receptors between HbAA and HbSS mice (Figure 5F).

**Effect of ET<sub>A</sub> receptor inhibition on Nav1.8 expression and channel activity in SCD DRG**

Previous studies have shown that ET-1 can alter the activity of TTX-R sodium channels in rat DRG neurons.<sup>26</sup> Nav1.8, a TTX-R sodium channel in DRG, participates in

chronic inflammatory pain genesis.<sup>27</sup> We first determined if Nav1.8 expression differed between HbAA and HbSS DRG. The levels of *Scn10a* mRNA (encoding Nav1.8) and *Scn11a* mRNA (encoding Nav1.9, another TTX-R sodium channel) were elevated in HbSS DRG (Figure 6A). The amount of Nav1.8 protein and the percentage of Nav1.8-positive neurons were also increased in HbSS DRG (Fig. 6 B, C). Four days of hindpaw ABT-627 administration abolished the increase in Nav1.8 protein in HbSS DRG (Figure 6 B), indicating that increased Nav1.8 requires ET<sub>A</sub> receptor activation in SCD (HbSS) DRG.

Furthermore, we analyzed Nav1.8 activity in HbSS DRG neurons. Whole cell voltage-clamp recordings were performed in freshly dissociated small DRG neurons since Nav1.8 is expressed predominantly in small DRG neurons.<sup>28</sup> Neurons were held at -60 mV, given a depolarizing step at 50 ms from -55 mV to +40 mV with a 5 mV increment (Figure 7A). Under this protocol with the presence of 500 nM TTX, Nav1.9 current was inhibited to keep the Nav1.8 current integrated.<sup>29</sup> Nav1.8 current density from the HbSS DRG neurons significantly increased compared to HbAA DRG neurons (Figure 7A, B). Bilateral subcutaneous ABT-627 administered daily over 4 days prior to DRG collection produced a larger reduction in Nav1.8 current density in HbSS DRG compared to HbAA DRG (Figure 7A, B). When tested at -15 mV, ABT-627 reduced Nav1.8 current by approximately 300 pA in HbSS DRG neurons, with no change in the HbAA DRG neurons

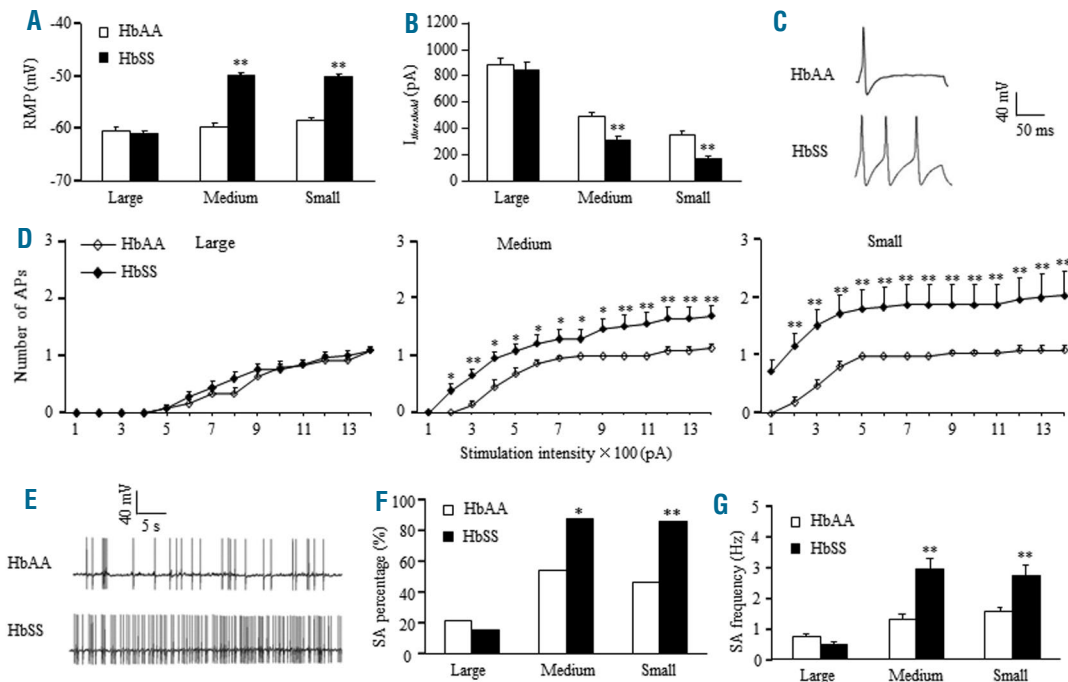


**Figure 2. Townes HbSS DRG neurons display increased excitability and spontaneous activity.** (A and B) Resting membrane potential (RMP, A) and current threshold for pulse ( $I_{\text{threshold}}$ , B). n = 24 large, 22 medium, and 21 small neurons from the HbAA group (7 mice). n = 25 large, 23 medium, and 25 small neurons from the HbSS group (6 mice). \*\* $P < 0.01$  vs. the corresponding HbAA group. (C) Representative trace of evoked action potentials in small DRG neurons. (D) Numbers of evoked action potentials (APs) in large, medium, and small DRG neurons from the HbAA and HbSS groups after application of different currents as indicated. Numbers of the recorded neurons are the same as in A. \* $P < 0.05$ , \*\* $P < 0.01$  vs. the same stimulation intensity in the HbAA group. (E) Representative trace of spontaneous activity in small DRG neurons from the HbAA and HbSS groups. (F and G) Percentage of DRG neurons that had spontaneous activity (SA, F) and frequency of spontaneous activity (G). n = 23 large, 22 medium, and 25 small DRG neurons for the HbAA group (7 mice). n = 26 large, 25 medium, and 22 small DRG neurons from the HbSS group (6 mice). \* $P < 0.05$ , \*\* $P < 0.01$  vs. the corresponding HbAA group.

(Figure 7C). These data further indicate that the increase in Nav1.8 current from HbSS DRG neurons is  $ET_A$  receptor-dependent. We also examined the gating properties of Nav1.8 in HbSS DRG neurons. HbSS DRG neurons showed a hyperpolarizing potential shift compared to HbAA DRG neurons under the conditions of either activation or inactivation of Nav1.8 (Figure 7 D, E). The half-maximal activation voltage ( $V_{1/2}$ ) was  $-20.35 \pm 1.16$  mV in the HbAA mice and  $-24.79 \pm 0.93$  mV in the HbSS mice (Figure 7D), whereas the half-maximal inactivation voltage ( $V_{1/2}$ ) was  $-37.56 \pm 1.32$  mV in the HbAA mice and  $-45.80 \pm 1.80$  mV in the HbSS mice (Figure 7E). *In vivo*

administration of ABT-627 as described above did not lead to changes in the gating properties of Nav1.8 in HbAA or HbSS mice. HbSS DRG neurons likely display  $ET_A$  receptor-independent changes in the gating properties of Nav1.8 channels.

### NF- $\kappa$ B-triggered Nav1.8 expression in HbSS DRG neurons

How does  $ET_A$  receptor activation mediate an increase in Nav1.8 expression and activity in SCD (HbSS) DRG neurons? The transcription factor, NF- $\kappa$ B, may be upstream of Nav1.8 upregulation in DRG neurons and is

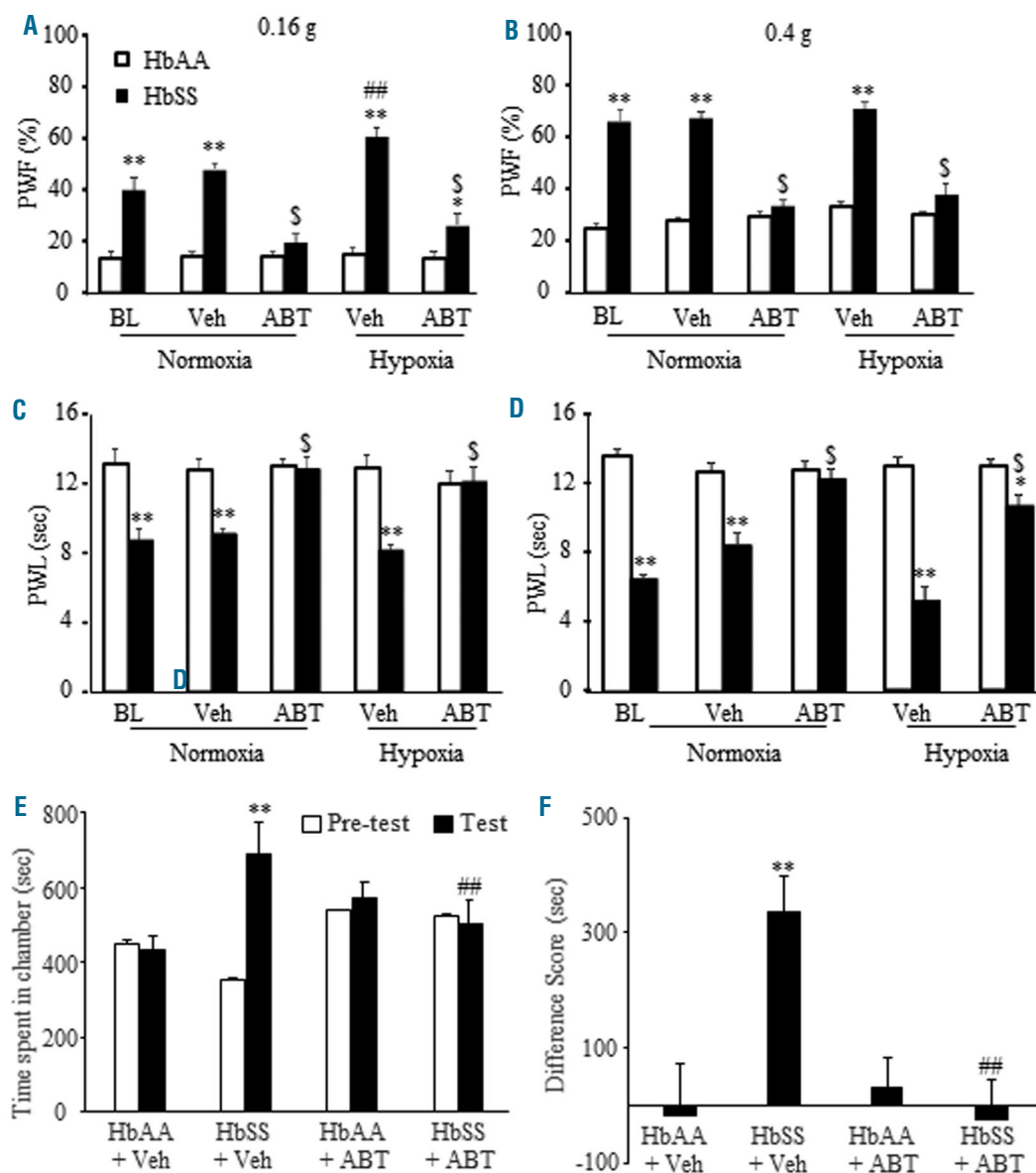


**Figure 3. Hindpaw administration of ABT-627 can alleviate pain hypersensitivity and spontaneous ongoing pain under normoxic and hypoxic conditions in male HbSS mice.** (A-D) Effect of hindpaw injection of ABT-627 on paw withdrawal frequencies (PWF) to a 0.16 g low force (A) and a 0.4g medium force (B) and paw withdrawal latencies (PWL) to heat (C) and cold (D) stimuli on the ipsilateral side of HbAA mice and HbSS mice under normoxic and hypoxic conditions. Veh: vehicle. ABT: ABT-627. n=6 mice/genotype/treatment. \* $P < 0.05$ , \*\* $P < 0.01$  vs. the corresponding HbAA group. ## $P < 0.01$  vs. the HbSS baseline value. \$ $P < 0.05$  vs. the corresponding vehicle-treated HbSS group. (E and F) Effect of hindpaw injection of ABT-627 (ABT) on ongoing pain as assessed by the conditioned place preference paradigm. n=6-8 mice/group. \*\* $P < 0.01$  vs. the corresponding pre-conditioning (E) or the HbAA plus vehicle (Veh) group (F). ## $P < 0.01$  vs. the corresponding post-conditioning (post) from the HbSS plus vehicle group or the HbSS plus vehicle group (F).

activated by ET-1.<sup>30,31</sup> To confirm this relationship among ET-1, ET<sub>A</sub> receptors, and Nav1.8 channels in DRG neurons, we cultured HbAA DRG neurons in the presence of ET-1 peptide. ET-1 stimulation of HbAA DRG neurons for 24 hours resulted in increases in the levels of Nav1.8 protein (Figure 8A) and phosphorylated p65 protein (an indicator of NF-κB activation<sup>32</sup>), a NF-κB subunit (Figure 8B). Co-incubation with ABT-627 or pyrrolidine dithiocarbamate (PDTC), an NF-κB-specific inhibitor, prevented these increases (Figure 8A and 8B). Furthermore, we examined the expression of phosphorylated p65 in *in vivo* mice injected intraperitoneally (i.p) with vehicle or ABT-627 once daily for 4 days. Phosphorylated p65 levels in HbSS DRG significantly increased after vehicle injection, but did not significantly change after ABT-627 administration compared to that in the HbAA mice after vehicle injection (Figure 8C). Total p65 protein levels did not significantly differ among treatment groups (Figure 8C). These findings indicate that NF-κB activation and Nav1.8 upregulation in HbSS DRG are ET<sub>A</sub> receptor-dependent and may be involved in SCD-associated pain. This conclusion is fur-

ther supported by our behavioral observations that single i.p administration of PDTC, a specific inhibitor of NF-κB activation, or A-803467, a specific antagonist of Nav1.8,<sup>33</sup> alleviated mechanical allodynia and/or thermal hyperalgesia in HbSS mice, without affecting the basal responses of HbAA mice (Figure 8D; *Online Supplementary Figure S10*).

We then examined whether activated NF-κB is directly linked to increased Nav1.8 expression in HbSS DRG. Using ChIP analyses, a fragment within the *Scn10a* promoter was amplified from a complex immunoprecipitated with an anti-p65 antibody (Figure 8E), indicating the binding of p65 to the *Scn10a* gene promoter in the DRG. This binding activity increased in the HbSS DRG compared to HbAA DRG, as shown by a 7-fold increase in band density (Figure 8E). To examine whether NF-κB activation directly regulates *Scn10a* transcriptional activity, we performed a dual luciferase assay using a mouse neuronal cell line (CAD cells)<sup>34</sup> transfected with a luciferase reporter vector containing the *Scn10a* gene promoter. Since phorbol 12-myristate 13-acetate (PMA) can activate NF-κB through protein kinase C (PKC) activation,<sup>35</sup> we applied

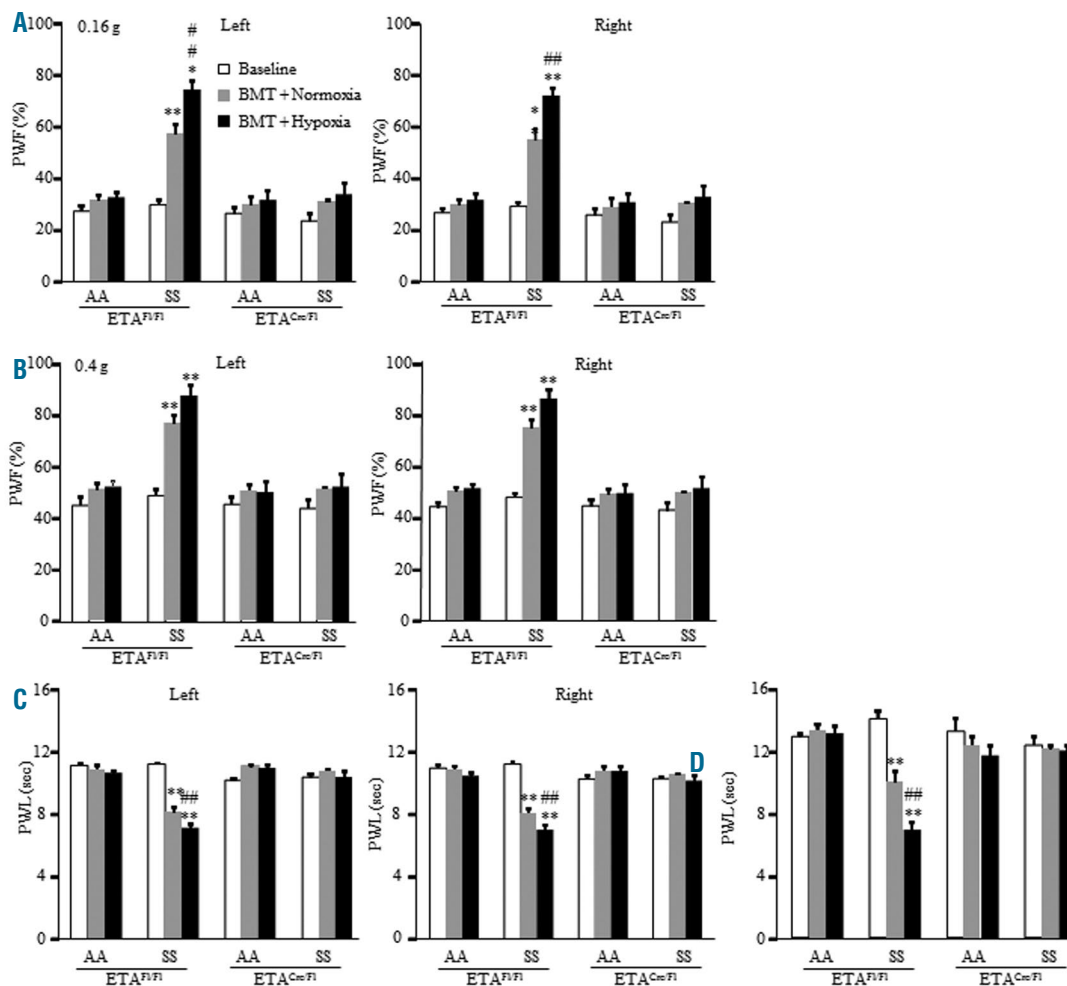


**Figure 4. Male HbSS mice with conditional genetic knockdown of DRG ET<sub>A</sub> receptors fail to develop pain hypersensitivity before and after hypoxia/reoxygenation exposure.** Paw withdrawal frequency (PWF) in response to a 0.16 g low mechanical force (A) and a 0.4 g medium mechanical force (B) and paw withdrawal latency (PWL) in response to heat (C) and cold (D) stimuli on both left and right sides of ET<sup>+/+</sup> mice and ET<sup>Cre/+</sup> mice 2 months after BerkSS (SS) or BerkAA (AA) bone marrow transplantation (BMT). n = 6-8 mice/group. \*\*P<0.01 vs. the corresponding baseline value. ###P<0.01 vs. the corresponding BMT + Normoxia value.

PMA into the medium. PMA stimulation increased the activity of the *Scn10a* gene promoter by 3.5-fold as compared to the vehicle-treated group (Figure 8F). Co-administration of PDTC or bisindolylmaleimide I (BIM), a PKC inhibitor, prevented this increase (Figure 8F). BIM or PDTC alone did not affect basal luciferase activity (Figure 8F). These results indicate that the increased *Scn10a* gene activity is a specific response to PKC/NF- $\kappa$ B activation. Single-cell RT-PCR analysis revealed that 40% of individual small DRG neurons co-expressed *Scn10a* mRNA, *Ednra* mRNA, and *Rela* mRNA (encoding p65) (Figure 8G). Taken together, our findings suggest the participation of NF- $\kappa$ B in ET<sub>A</sub> receptor-dependent Nav1.8 upregulation in HbSS DRG neurons (Online Supplementary Figure S11).

## Discussion

Pain is a major symptom reported by SCD patients. Currently, painkillers such as opioids are prescribed for SCD pain management but repeated and/or prolonged administration of these drugs has limited analgesic efficacy and the potential to produce side effects.<sup>6</sup> Identifying novel and specific targets for pain management is essential for improving SCD patient care. We showed here that the expression of ET-1 and its ET<sub>A</sub> receptor increases in the DRG of SCD mice. Sensory neuron-specific knockdown or local inhibition of DRG ET<sub>A</sub> receptors alleviated basal and post-hypoxia mechanical allodynia and thermal/cold hyperalgesia in SCD mice. Although the exact mechanism

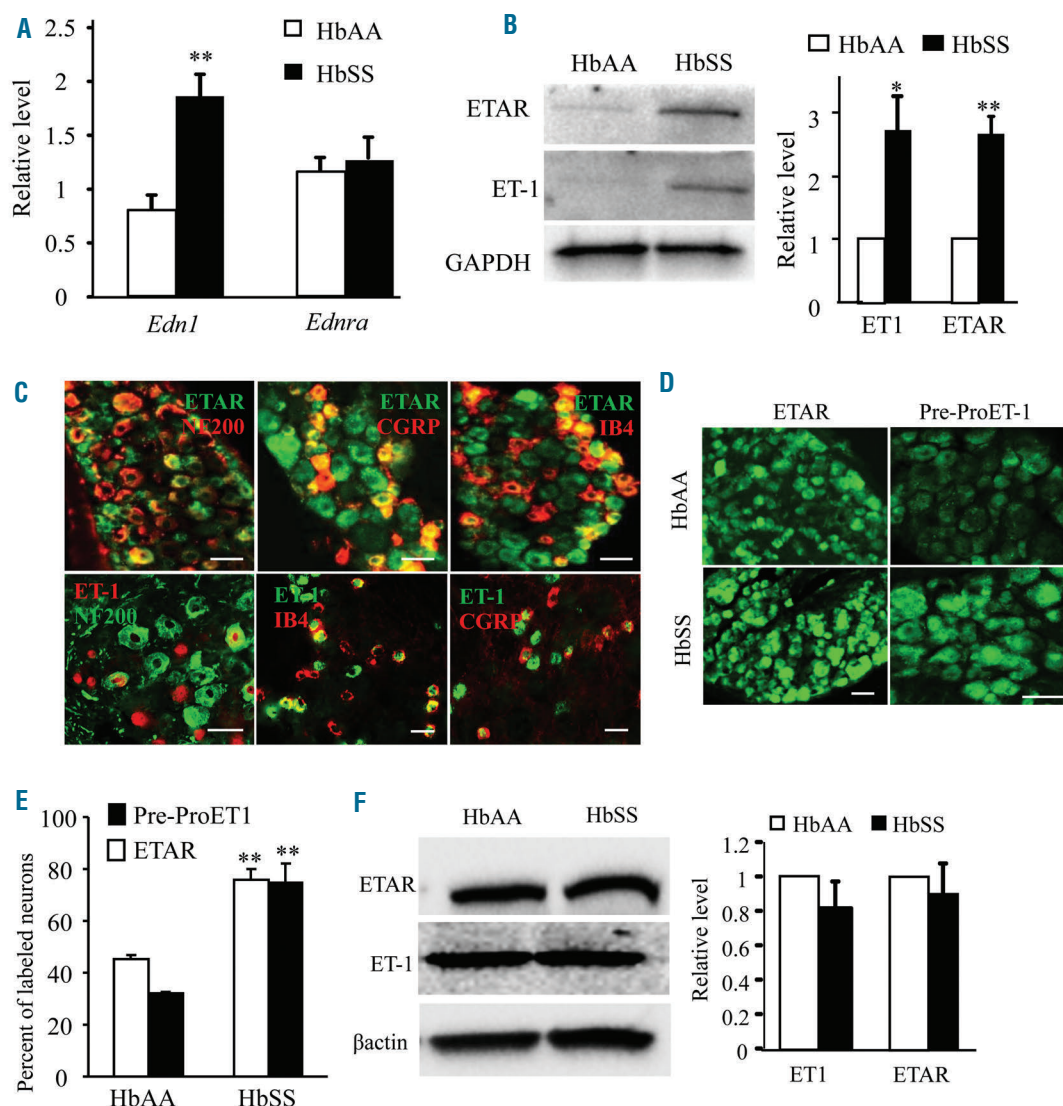


**Figure 5. ET-1 and ET<sub>A</sub> receptor expression increases in the DRG of Townes HbSS mice.** (A) Expression of *Edn1* mRNA (encoding ET-1) and *Ednra* mRNA (encoding ET<sub>A</sub> receptor) in the L3-L4 DRG. n=3 mice/genotype. \*\**P*<0.01 vs. the corresponding HbAA mice. (B) Expression of ET-1 and ET<sub>A</sub> receptor proteins in the L3-L4 DRG. Left: representative Western blots. Right: a summary of densitometric analysis. n=3 mice/genotype. \**P*<0.05 and \*\**P*<0.01 vs. the corresponding HbAA mice. (C) Double immunostaining shows the co-localization of ET<sub>A</sub> receptors (ETAR) or pre-pro ET-1 (ET-1) with CGRP, IB4, and NF200 in the L3-L4 DRG of HbAA mice (for ETAR) or HbSS mice (for ET-1). Scale bar: 50  $\mu$ m. (D and E) Number of ET<sub>A</sub> receptors (ETAR)-positive neurons or pre-pro ET-1 (ET-1)-positive neurons in the L4 DRG from HbAA mice and HbSS mice. D: representative immunostaining images. E: a summary of statistical analysis of the number of positive neurons. n=3 mice/genotype. \*\**P*<0.01 vs. the HbAA mice. Scale bar: 50  $\mu$ m. (F) Expression of ET-1 and ET<sub>A</sub> receptor proteins in hind paw from HbAA mice and HbSS mice. Left: representative Western blots. Right: a summary of densitometric analysis. n=3 mice/genotype.

underlying these effects requires further validation in SCD mouse models, our study suggests that ET<sub>A</sub> receptors are key players in SCD-associated pain.

The present study used two humanized mouse models of SCD, the Berkeley and Townes, to analyze SCD-associated pain. Although pain-like behaviors in SCD mouse models may not exactly mimic pain in SCD patients due to several confounding environmental and emotional variables, analyzing pain hypersensitivity in SCD murine models is a productive tool for identifying the underlying mechanisms of SCD-associated pain. These mice displayed significant mechanical allodynia, thermal/cold hyperalgesia, and spontaneous ongoing pain consistent with previous reports.<sup>36</sup> Using age-matched male and female HbSS and HbAA littermates, we found no significant sex-based differences in basal or post-hypoxia evoked pain hypersensitivity or ABT-627 efficacy. This aligns with clinical reports that found no significant differences in self-reported pain experiences between male and female SCD patients.<sup>37,38</sup> Interestingly, Townes HbSS mice did not display a similar degree of pain exacerbation following hypoxia/reoxygenation compared to the BerkSS mice. This may be related to the presence of a human  $\beta$ -globin locus control region (LCR) that leads to hemoglobin switching similar to humans in the Townes HbSS mice, although both models express human globins. In the Townes model, relative  $\gamma$ -globin expression ( $\gamma/\gamma+\beta S$ ) at birth is between 30% to 50%, then  $\beta$ -globin expression dominates at 1 month of age.<sup>39</sup> In contrast, the Berkeley model exhibits a complete  $\gamma$ -globin to  $\beta$ -globin switch in utero leading to greater prenatal death and low birth rates. Given that higher  $\gamma$ -globin expression is associated with diminished SCD symptoms,<sup>40</sup> the early expression of  $\beta$ -globin in BerkSS mice may cause more severe symptoms of SCD, which could explain their significant pain exacerbation following hypoxia/reoxygenation.

An increase in ET<sub>A</sub> receptor expression may be attributed to the elevated ET-1 in the DRG neurons of HbSS

mice. The levels of ET-1 mRNA, ET-1 protein, and ET<sub>A</sub> receptor protein increased in HbSS DRG. Consistent with previous studies,<sup>10,25</sup> ET-1 and ET<sub>A</sub> receptors are predominantly expressed in DRG neurons, although ET-1 expression in immune cells found in HbSS DRG cannot be ruled out.<sup>41</sup> Elevated ET-1 could trigger increased ET<sub>A</sub> receptor expression in DRG possibly through increased receptor cycling to the membrane and/or enhanced transcription or translation.<sup>42,43</sup> Since we found no significant changes in ET<sub>A</sub> receptor mRNA in HbSS DRG, it would be expected that, under constantly elevated ET-1 conditions, ET-1/ET<sub>A</sub> receptor cycling coupled with ET-1-triggered activation of intracellular signals enhances ET<sub>A</sub> receptor translation through unknown mechanisms in HbSS DRG. The mechanism of ET<sub>A</sub> receptor upregulation in HbSS DRG remains to be further investigated.

ET<sub>A</sub> receptors are required for increased Nav1.8 expression in HbSS DRG, since ET<sub>A</sub> receptor inhibition completely blocked increases in Nav1.8 protein and current in HbSS DRG. However, whether the participation of DRG ET<sub>A</sub> receptors in the pain hypersensitivity of HbSS mice is mediated by DRG Nav1.8 upregulation in HbSS mice requires further investigation as the present data showed only an association between activation of the ET<sub>A</sub> receptors and upregulation of Nav1.8 in the DRG of HbSS mice. Interestingly, ET<sub>A</sub> receptor inhibition did not alleviate the hyperpolarizing shift in the gating properties of Nav1.8 channels in HbSS DRG. Previous studies reported that phosphorylation of Nav1.8 channels by protein kinase A (PKA), but not PKC, could affect the channel's gating properties.<sup>44,45</sup> The altered gating of Nav1.8 channels in the HbSS DRG is likely the result of activation of PKA by an ET<sub>A</sub> receptor-independent signaling mechanism. It is worth noting that the leftward shift of 4.44 mV in the HbSS DRG would only result in a modest increase in sodium current.<sup>26</sup> Given that ABT-627 fully attenuated the increase in Nav1.8 current in the HbSS DRG, an ET<sub>A</sub>-receptor independent mechanism of Nav1.8 channel

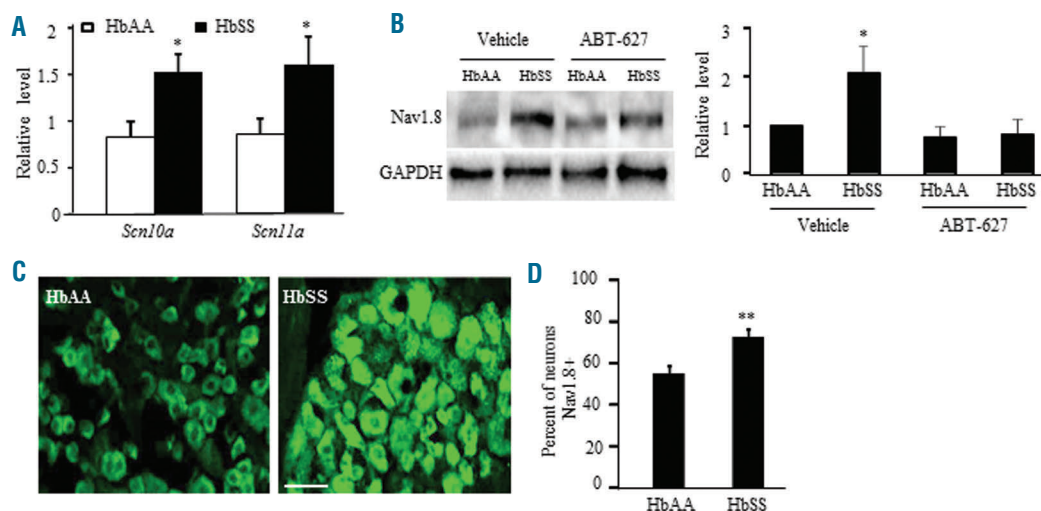


**Figure 6. Nav1.8 expression is elevated in Townes HbSS DRG and is ET<sub>A</sub> receptor-dependent.** (A) Expression of *Scn10a* mRNA (encoding Nav1.8) and *Scn11a* mRNA (encoding Nav1.9) in the L3-L4 DRG from HbAA mice and HbSS mice. n=3 mice/genotype. \**P*<0.05 vs. the corresponding HbAA mice. (B) Effect of hindpaw injection of ABT-627 or vehicle on expression of Nav1.8 protein in the L3-L4 DRG from HbAA mice and HbSS mice. Left: representative Western blots. Right: a summary of densitometric analysis. n=3 mice/group. \**P*<0.05 vs. the vehicle-treated HbAA mice. (C) Number of Nav1.8-labeled neurons in the L4 DRG from HbAA mice and HbSS mice. Left: representative immunostaining images. Right: a summary of statistical analysis of the number of Nav1.8-labeled neurons. Scale bar: 50  $\mu$ m. n = 3 mice/genotype. \*\**P*<0.01 vs. the HbAA mice.



phosphorylation may not be a significant contributor to Nav1.8-mediated neuronal excitability and behavioral pain hypersensitivity. Additionally, we observed that the resting membrane potential of HbSS DRG neurons was elevated. This suggests a possible decrease in potassium channel expression or function. ET-1 has been shown to depress delayed rectifier potassium currents in rat DRG neurons.<sup>46</sup> This depression of potassium currents may be involved in increased excitability of SCD neurons and the pain hypersensitivity of SCD mice found in this study. Thus, it is of interest to further examine whether the expression of other ion channels including delayed rectifi-

er potassium channels differs between HbAA and HbSS DRG neurons and whether these differences are  $ET_A$  receptor-dependent.

NF- $\kappa$ B may be a key modulator of  $ET_A$  receptor-dependent Nav1.8 upregulation in HbSS DRG. NF- $\kappa$ B is expressed in small and medium neurons of the DRG.<sup>47</sup> Under inflammatory conditions, PKC $\epsilon$  activation has been linked to Nav1.8 upregulation in DRG neurons<sup>48</sup> and NF- $\kappa$ B activation.<sup>49</sup> A recent study also reported that chemokine ligand 2 can induce NF- $\kappa$ B activation via PKC and lead to Nav1.8 upregulation in DRG neurons.<sup>30</sup> Since  $ET_A$  receptor activation leads to the downstream activa-

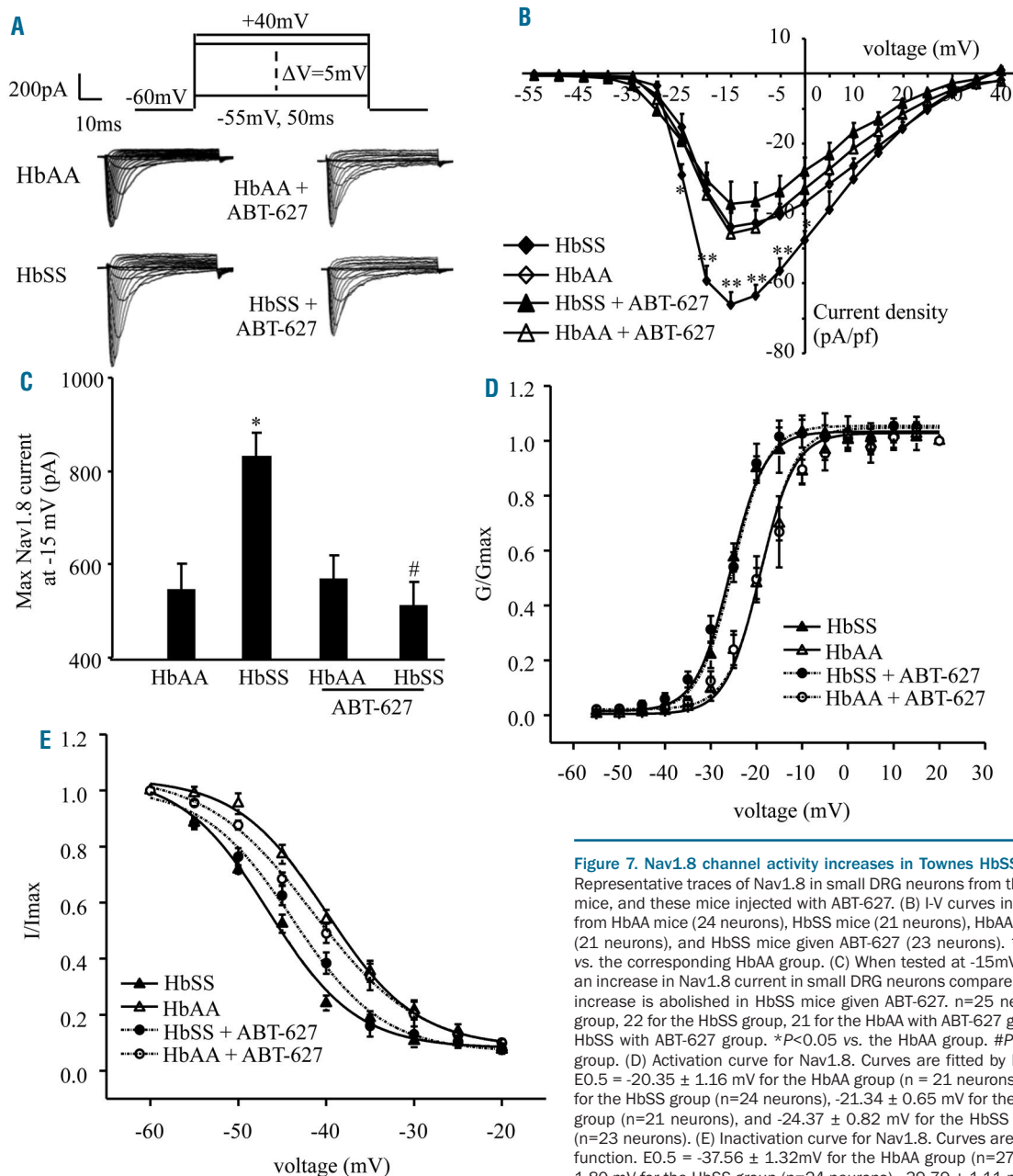


**Figure 7. Nav1.8 channel activity increases in Townes HbSS DRG neurons.** (A) Representative traces of Nav1.8 in small DRG neurons from the HbAA mice, HbSS mice, and these mice injected with ABT-627. (B) I-V curves in small DRG neurons from HbAA mice (24 neurons), HbSS mice (21 neurons), HbAA mice given ABT-627 (21 neurons), and HbSS mice given ABT-627 (23 neurons). \* $P < 0.05$ , \*\* $P < 0.01$  vs. the corresponding HbAA group. (C) When tested at -15mV, HbSS mice exhibit an increase in Nav1.8 current in small DRG neurons compared to HbAA mice. This increase is abolished in HbSS mice given ABT-627.  $n = 25$  neurons for the HbAA group, 22 for the HbSS group, 21 for the HbAA with ABT-627 group, and 23 for the HbSS with ABT-627 group. \* $P < 0.05$  vs. the HbAA group. # $P < 0.05$  vs. the HbSS group. (D) Activation curve for Nav1.8. Curves are fitted by Boltzmann function.  $E_{0.5} = -20.35 \pm 1.16$  mV for the HbAA group ( $n = 21$  neurons),  $-24.79 \pm 0.93$  mV for the HbSS group ( $n = 24$  neurons),  $-21.34 \pm 0.65$  mV for the HbAA with ABT-627 group ( $n = 21$  neurons), and  $-24.37 \pm 0.82$  mV for the HbSS with ABT-627 group ( $n = 23$  neurons). (E) Inactivation curve for Nav1.8. Curves are fitted by Boltzmann function.  $E_{0.5} = -37.56 \pm 1.32$  mV for the HbAA group ( $n = 27$  neurons),  $-45.80 \pm 1.80$  mV for the HbSS group ( $n = 24$  neurons),  $-39.79 \pm 1.11$  mV for the HbAA with ABT-627 group ( $n = 19$  neurons), and  $-41.05 \pm 1.86$  mV for the HbSS with ABT-627 group ( $n = 24$  neurons).

tion of PKC $\epsilon$  and PKC $\delta$ ,<sup>50</sup> it is likely that ET<sub>A</sub> receptors contribute to increased Nav1.8 expression through NF- $\kappa$ B activation in HbSS DRG. NF- $\kappa$ B activation was indeed enhanced in ET-1-stimulated cultured DRG neurons and *in vivo* HbSS DRG, and this enhanced activation was ET<sub>A</sub> receptor-dependent. NF- $\kappa$ B binding to the *Scn10a*

(Nav1.8) promoter region increased in HbSS DRG. Additionally, PKC-induced NF- $\kappa$ B activation led to increased *Scn10a* promoter activity in mouse neuronal cells. These findings suggest that the Nav1.8 upregulation found in HbSS DRG is the result of ET-1/ET<sub>A</sub> receptor-induced NF- $\kappa$ B activation. However, the involvement of

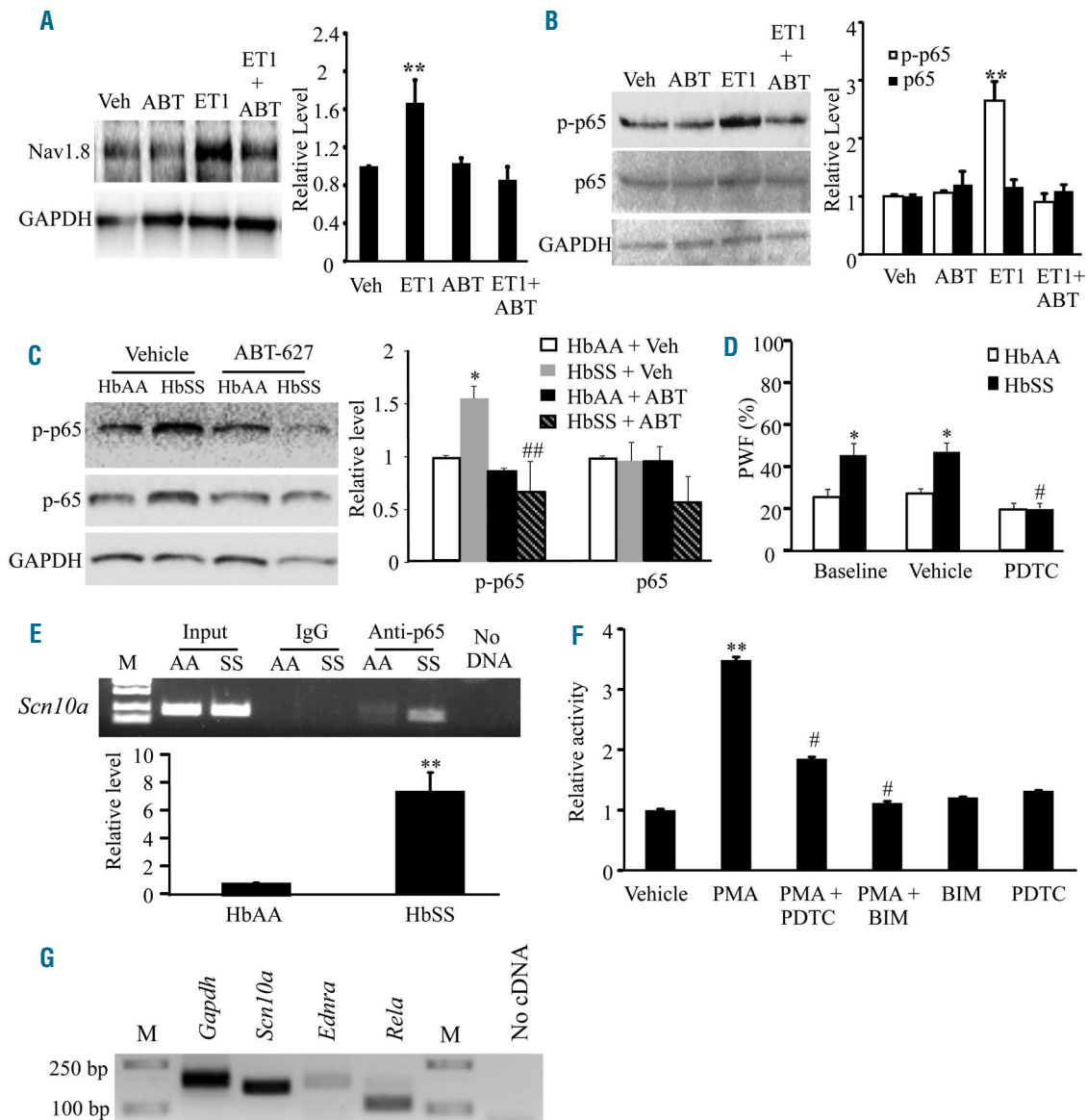


**Figure 8. ET-1 induced activation of ET<sub>A</sub> receptors leads to the upregulation of Nav1.8 and activation of NF- $\kappa$ B in HbSS DRG neurons.** (A) Cultured HbAA DRG neurons exposed to 400 nmol of ET-1 peptide for 24 hr displayed an increase in Nav1.8 protein. Co-administration of ABT-627 (1  $\mu$ mol) prevented this increase. Left: Representative western blots. Right: Summary of densitometric analysis. n=3 biological repeats. \*\**P*<0.01 vs. the vehicle (Veh) group. (B) Cultured HbAA DRG neurons exposed to 400 nmol of ET-1 peptide for 90 minutes displayed an increase in phosphorylated p65 (p-p65). Co-administration of ABT-627 (1  $\mu$ mol) 10 minutes prior to ET-1 stimulation prevented the increase in phosphorylated p65 protein. Left: Representative western blots. Right: Summary of densitometric analysis n=3 biological repeats. \*\**P*<0.01 vs. the vehicle (Veh) group. (C) The levels of phosphorylated p65 (p-p65), increase in the L3-L4 DRG of the vehicle-treated HbSS mice. This increase is not seen in the ABT-627-treated HbSS mice. Left: representative Western blots. Right: a summary of densitometric analysis. n=3 mice/group. \**P*<0.01 vs. the vehicle-treated HbAA group, ##*P*<0.01 vs. the vehicle-treated HbSS group. (D) 45 mins after intraperitoneal injection of the NF- $\kappa$ B-specific inhibitor, PDTC, increased response to a low force (0.16 g) von Frey filament is alleviated in the HbSS mice. n = 6 mice/group. \**P*<0.05 vs. the baseline in HbAA mice. #*P*<0.05 vs. the baseline in HbSS mice. (E) *Scn10a* promoter fragments immunoprecipitated by rabbit anti-p65 in the L3-L5 DRG from HbSS (SS) and HbAA (AA) mice. Top: representative gel image. Bottom: a summary of densitometric analysis. Input: total purified fragments. M: ladder marker. n=3 mice/genotype. \*\**P*<0.01 vs. the HbAA mice. (F) *Scn10a* promoter activity in mouse CAD cells transfected with a luciferase reporter vector containing a *Scn10a* promoter and treated with drugs as indicated. PMA: the PKC activator. BIM: the PKC-specific inhibitor. PDTC: the NF- $\kappa$ B-specific inhibitor. n=3 repeats/treatment. One-way ANOVA on Ranks. \*\**P*<0.01 vs. the vehicle group. #*P*<0.05 vs. the PMA-treated group. (G) Single cell RT-PCR analysis shows the co-expression of *Scn10a* mRNA, *Ednra* mRNA (encoding ET-1), and *Rela* mRNA (encoding p65) in individual small DRG neurons from HbAA mice. *Gapdh* mRNA is used as a positive control. M: ladder marker. n=3 repeats.

other transcription factors or molecules in ET-1/ET<sub>A</sub> receptor-mediated Nav1.8 upregulation in HbSS DRG could not be excluded.

In conclusion, this study provides evidence for one possible mechanism by which ET-1/ET<sub>A</sub> receptors contribute to SCD-associated pain likely through the NF-κB-triggered upregulation of Nav1.8 in primary sensory neurons. We identified the ability of ABT-627, an ET<sub>A</sub> receptor-specific antagonist,<sup>24</sup> to alleviate basal and post-hypoxia evoked pain hypersensitivity in SCD mice. At the dosages used, ABT-627 produced pain relief that persisted for the entire testing period (at least 7 hours) with no noticeable side effects. Given that ABT-627 and similar

ET<sub>A</sub> receptor antagonists have been used in phase II/III clinical trials for cancer treatment<sup>18,19</sup> and are beneficial for SCD-related pulmonary hypertension,<sup>16</sup> targeting DRG ET<sub>A</sub> receptors may have potential therapeutic value for SCD-associated pain management.

### Funding

This work was supported by NIH grants (R01NS094664, R01NS094224, R01DA033390, and U01HL117684) to YXT and by a NIH research Fellowship (F31NS092310) to BML at Rutgers New Jersey Medical School. We thank Dr. Roger Howell at Rutgers New Jersey Medical School for his assistance with animal radiation.

### References

- Bunn HF. Pathogenesis and Treatment of Sickle Cell Disease. *N Engl J Med.* 1997;337(11):762-769.
- Brozovic M, Davies S. Management of sickle cell disease. *Postgrad Med J.* 1987;63(742):605-609.
- Manwani D, Frenette PS. Vaso-occlusion in sickle cell disease: pathophysiology and novel targeted therapies. *Hematology Am Soc Hematol Educ Program.* 2013;2013:362-369.
- Smith WR, Penberthy LT, Bovbjerg VE, et al. Daily assessment of pain in adults with sickle cell disease. *Ann Intern Med.* 2008;148(2):94-101.
- Brandow AM, Farley RA, Panepinto JA. Neuropathic pain in patients with sickle cell disease. *Pediatr Blood Cancer.* 2014;61(3):512-517.
- Gupta M, Msambichaka L, Ballas SK, Gupta K. Morphine for the treatment of pain in sickle cell disease. *ScientificWorldJournal.* 2015;2015:540154.
- Chichorro JG, Fiuzza CR, Bressan E, Claudino RF, Leite DF, Rae GA. Endothelins as pronociceptive mediators of the rat trigeminal system: Role of ETA and ETB receptors. *Brain Res.* 2010;1345:73-83.
- Barr TP, Kam S, Khodorova A, Montmayeur JP, Strichartz GR. New perspectives on the endothelin axis in pain. *Pharmacol Res.* 2011;63(6):532-540.
- Ergul S, Brunson CY, Hutchinson J, et al. Vasoactive factors in sickle cell disease: In vitro evidence for endothelin-1-mediated vasoconstriction. *Am J Hematol.* 2004;76(3):245-251.
- Pomonis JD, Rogers SD, Peters CM, Ghilardi JR, Mantyh PW. Expression and localization of endothelin receptors: implications for the involvement of peripheral glia in nociception. *J Neurosci.* 2001;21(3):999-1006.
- Motta EM, Chichorro JG, Rae GA. Role of ETA and ETB endothelin receptors on endothelin-1-induced potentiation of nociceptive and thermal hyperalgesic responses evoked by capsaicin in rats. *Neurosci Lett.* 2009;457(3):146-150.
- Gokin AP, Fareed MU, Pan HL, Hans G, Strichartz GR, Davar G. Local injection of endothelin-1 produces pain-like behavior and excitation of nociceptors in rats. *J Neurosci.* 2001;21(14):5358-5366.
- Graido-Gonzalez E, Doherty JC, Bergreen EW, Organ G, Telfer M, McMillen MA. Plasma endothelin-1, cytokine, and prostaglandin E2 levels in sickle cell disease and acute vaso-occlusive sickle crisis. *Blood.* 1998;92(7):2551-2555.
- Rybicki AC, Benjamin LJ. Increased levels of endothelin-1 in plasma of sickle cell anemia patients. *Blood.* 1998;92(7):2594-2596.
- Heimlich JB, Speed JS, O'Connor PM, et al. Endothelin-1 contributes to the progression of renal injury in sickle cell disease via reactive oxygen species. *Br J Pharmacol.* 2016;173(2):386-395.
- Minniti CP, Machado RF, Coles WA, Sachdev V, Gladwin MT, Kato GJ. Endothelin receptor antagonists for pulmonary hypertension in adult patients with sickle cell disease. *Br J Haematol.* 2009;147(5):737-743.
- Zappia KJ, Garrison SR, Hillery CA, Stucky CL. Cold hypersensitivity increases with age in mice with sickle cell disease. *Pain.* 2014;155(12):2476-85.
- Carducci MA, Manola J, Nair SG, et al. Atrasentan in patients with advanced renal cell carcinoma: a phase II trial of the ECOG-ACRIN Cancer Research Group (E6800). *Clin Genitourin Cancer.* 2015;13(6):531-539.
- Quinn DJ, Tangen CM, Hussain M, et al. Docetaxel and atrasentan versus docetaxel and placebo for men with advanced castration-resistant prostate cancer (SWOG S0421): a randomised phase 3 trial. *Lancet Oncol.* 2013;14(9):893-900.
- Cain DM, Vang D, Simone DA, Hebbel RP, Gupta K. Mouse models for studying pain in sickle disease: effects of strain, age, and acuteness. *Br J Haematol.* 2012;156(4):535-544.
- Cataldo G, Rajput S, Gupta K, Simone DA. Sensitization of nociceptive spinal neurons contributes to pain in a transgenic model of sickle cell disease. *Pain.* 2015;156(4):722-730.
- Zhao JY, Liang L, Gu X, et al. DNA methyltransferase DNMT3a contributes to neuropathic pain by repressing Kcna2 in primary afferent neurons. *Nat Commun.* 2017; 8, 14712.
- Turhan A, Weiss LA, Mohandas N, Coller BS, Frenette PS. Primary role for adherent leukocytes in sickle cell vascular occlusion: A new paradigm. *Proc Natl Acad Sci USA.* 2002;99(5):3047-3051.
- Jarvis MF, Wessale JL, Zhu CZ, et al. ABT-627, an endothelin ET(A) receptor-selective antagonist, attenuates tactile allodynia in a diabetic rat model of neuropathic pain. *Eur J Pharmacol.* 2000;388(1):29-35.
- Stosser S, Agarwal N, Tappe-Theodor A, Yanagisawa M, Kuner R. Dissecting the functional significance of endothelin A receptors in peripheral nociceptors in vivo via conditional gene deletion. *Pain.* 2010;148(2):206-214.
- Zhou Z, Davar G, Strichartz G. Endothelin-1 (ET-1) selectively enhances the activation gating of slowly inactivating tetrodotoxin-resistant sodium currents in rat sensory neurons: a mechanism for the pain-inducing actions of ET-1. *J Neurosci.* 2002;22(15):6325-6330.
- Joshi SK, Mikusa JP, Hernandez G, et al. Involvement of the TTX-resistant sodium channel Nav 1.8 in inflammatory and neuropathic, but not post-operative, pain states. *Pain.* 2006;123(1-2):75-82.
- Wang W, Gu J, Li YQ, Tao YX. Are voltage-gated sodium channels on the dorsal root ganglion involved in the development of neuropathic pain? *Mol Pain.* 2011;7:16.
- Gu XY, Liu BL, Zang KK, et al. Dexmedetomidine inhibits tetrodotoxin-resistant Nav1.8 sodium channel activity through Gi/o-dependent pathway in rat dorsal root ganglion neurons. *Mol Brain.* 2015;8:15.
- Zhao R, Pei GX, Cong R, Zhang H, Zang CW, Tian T. PKC-NF-κB are involved in CCL2-induced Nav1.8 expression and channel function in dorsal root ganglion neurons. *Biosci Rep.* 2014;34(3).
- Cianfrocca R, Tocci P, Semprucci E, et al. - Arrestin 1 is required for endothelin-1-induced NF-κB activation in ovarian cancer cells. *Life Sci.* 2014;118(2):179-184.
- Wang P, Qiu W, Dudgeon C, et al. PUMA is directly activated by NF-κB and contributes to TNF-α-induced apoptosis. *Cell Death Differ.* 2009;16(9):1192-1202.
- Jarvis MF, Honore P, Shieh CC, et al. A-803467, a potent and selective Nav1.8 sodium channel blocker, attenuates neuropathic and inflammatory pain in the rat. *Proc Natl Acad Sci USA.* 2007;104(20):8520-8525.
- Qi Y, Wang JKT, McMillan M, Chikaraishi DM. Characterization of a CNS cell line, CAD, in which morphological differentiation is initiated by serum deprivation. *J Neurosci.* 1997;17(4):1217-1225.
- Moscat J, Diaz-Meco MaT, Rennett P. NF-κB activation by protein kinase C isoforms and B-cell function. *EMBO Rep.* 2003;4(1):31-36.
- He Y, Wilkie DJ, Nazari J, et al. PKCδ-targeted intervention relieves chronic pain in a murine sickle cell disease model. *J Clin Invest.* 2016;126(8):3053-3057.
- Fosdal MB. Perception of pain among pediatric patients with sickle cell pain crisis. *J Pediatr Oncol Nurs.* 2014;32(1):5-20.
- McClish D, Levenson JL, Penberthy LT, et al. Gender differences in pain and health-

- care utilization for adult sickle cell patients: The PiSCES Project. *J Womens Health (Larchmt)*. 2006;15(2):146-154.
39. Ryan TM, Ciavatta DJ, Townes TM. Knockout-transgenic mouse model of sickle cell disease. *Science*. 1997;278(5339):873-876.
  40. Nevitt SJ, Jones AP, Howard J. Hydroxyurea (hydroxycarbamide) for sickle cell disease. *Cochrane Database Syst Rev*. 2017;4:CD002202.
  41. Ehrenreich H, Andereson RW, Fox CH, et al. Endothelins, peptides with potent vasoactive properties, are produced by human macrophages. *J Exp Med*. 1990; 172(6):1741-1748.
  42. Bremnes T, Paasche JD, Mehlum A, Sandberg C, Bremnes B, Attramadal H. Regulation and intracellular trafficking pathways of the endothelin receptors. *J Biol Chem*. 2000;275(23):17596-17604.
  43. Hansen-Schwartz J, Svensson CL, Xu CB, Edvinsson L. Protein kinase mediated upregulation of endothelin A, endothelin B and 5-hydroxytryptamine 1B/1D receptors during organ culture in rat basilar artery. *Br J Pharmacol*. 2002;137(1):118-126.
  44. Gold M, Levine J, Correa A. Modulation of TTX-R INa by PKC and PKA and their role in PGE2-induced sensitization of rat sensory neurons in vitro. *J Neurosci*. 1998;18(24):10345-10355.
  45. England S, Bevan S, Docherty RJ. PGE2 modulates the tetrodotoxin-resistant sodium current in neonatal rat dorsal root ganglion neurones via the cyclic AMP-protein kinase A cascade. *J Physiol*. 1996;495(Pt 2):429-440.
  46. Feng B, Strichartz G. Endothelin-1 raises excitability and reduces potassium currents in sensory neurons. *Brain Res Bull*. 2009; 79(6):345-350.
  47. Berti-Mattera LN, Larkin B, Hourmouzis Z, Kern TS, Siegel RE. NF- $\kappa$ B subunits are differentially distributed in cells of lumbar dorsal root ganglia in naive and diabetic rats. *Neurosci Lett*. 2011;490(1):41-45.
  48. Cang CL, Zhang H, Zhang YQ, Zhao ZQ. PKCepsilon-dependent potentiation of TTX-resistant Nav1.8 current by neurokinin-1 receptor activation in rat dorsal root ganglion neurons. *Mol Pain*. 2009;5:33.
  49. Satoh A, Gukovskaya AS, Nieto JM, et al. PKC- $\delta$  and - $\epsilon$  regulate NF- $\kappa$ B activation induced by cholecystokinin and TNF-alpha in pancreatic acinar cells. *Am J Physiol Gastrointest Liver Physiol*. 2004; 287(3):G582-591.
  50. Clerk A, Bogoyevitch MA, Anderson MB, Sugden PH. Differential activation of protein kinase C isoforms by endothelin-1 and phenylephrine and subsequent stimulation of p42 and p44 mitogen-activated protein kinases in ventricular myocytes cultured from neonatal rat hearts. *J Biol Chem*. 1994; 269(52):32848-32857.